engineering proceedings

Proceeding Paper

Impact of Gd_2O_3 Incorporation in Structural, Optical, Thermal, Mechanical, and Radiation Blocking Nature in HMO Boro-Tellurite Glasses †

Ashwitha Nancy D'Souza [1], M. I. Sayyed [2] and Sudha D. Kamath [1,*]

1 Department of Physics, Manipal Institute of Technology, Manipal Academy of Higher Education, Manipal 576104, India; nancyash983@gmail.com
2 Department of Physics, Faculty of Science, Isra University, Amman 11622, Jordan; drmabualssayed@gmail.com
* Correspondence: sudha.kamath@manipal.edu
† Presented at the IEEE 5th Eurasia Conference on Biomedical Engineering, Healthcare and Sustainability, Tainan, Taiwan, 2–4 June 2023.

Abstract: The glass system of B_2O_3-SiO_2-TeO_2-Bi_2O_3-ZnO-BaO doped with Gd_2O_3 (x = 0, 1, 2, 3, and 4 mol%) (BiTeGd-x) was prepared by using the melt-quench technique. The density of glasses increased from 5.323–5.579 g cm^{-3} for 0–4 mol% with an increase in Gd_2O_3 concentration. The simulation results obtained using Photon Shielding and Dosimetry (PSD) software (Phy-X version) produced the maximum mass attenuation coefficient (MAC) and minimum half-value layer (HVL) in the entire photon energy spectrum 0.015–15 MeV, suggesting the highest potential of BiTeGd-4 glass to act as a shield against low and high-energy radiation photons.

Keywords: Gd^{3+} ions; tellurite glass; radiation shielding; mass attenuation coefficient

check for updates

Citation: D'Souza, A.N.; Sayyed, M.I.; Kamath, S.D. Impact of Gd_2O_3 Incorporation in Structural, Optical, Thermal, Mechanical, and Radiation Blocking Nature in HMO Boro-Tellurite Glasses. *Eng. Proc.* **2023**, *55*, 97. https://doi.org/10.3390/engproc2023055097

Academic Editors: Teen-Hang Meen, Kuei-Shu Hsu and Cheng-Fu Yang

Published: 26 March 2024

1. Introduction

The usefulness of glass materials for protection against radiation has been extensively explored by researchers. Simple fabrication techniques, non-toxicity, transparency, chemical durability, and chemical flexibility are the main contributing factors of glasses to enhance radiation shielding proficiency and achieve high density [1]. Certain glasses designed have transcended conventional shielding materials such as concretes and bricks with appropriate attenuation coefficients and half-value layers (HVL). Tellurite glasses show promising results for thermal and chemical stability with a low melting temperature and density [2].

Rare-earth oxide such as Gd_2O_3 has been reported to improve the physical, optical, and mechanical properties of tellurite glasses by increasing their density, refractive index, and hardness values [3]. Kaewjaeng et al. [4] suggested that Gd^{3+} doping reduced HVT significantly, allowing the glass to perform better than commercial X-ray windows, concrete, and bricks [5]. There are limited investigations on the effect of Gd^{3+} ions and the overall improvement of the stability of glasses and radiation shielding properties. The present study was carried out to explore the potential of this glass system in radiation field application by analyzing the physical, optical, and radiation-blocking development of B_2O_3-SiO_2-Gd_2O_3-TeO_2-Bi_2O_3-ZnO-BaO glass system (BiTeGd-x).

2. Materials and Methods

Melt quenching was conducted to produce the BiTeGd-x system where Gd_2O_3 mol% varied as 0, 1, 2, 3, and 4. A furnace temperature of 1100–1120 °C was used for its synthesis [6]. The density of prepared glasses was determined using Archimedes theory and distilled water. Carl Zeiss FESEM recorder was used to study its surface morphology through EDAX measurement. Theoretical values of terms to evaluate the gamma-ray shielding property such as mass attenuation coefficient (MAC), and HVL of the synthesized glasses were obtained by using Photon Shielding and Dosimetry (PSD)(Phy-X version) software in an energy region of 0.015–15 MeV [7].

3. Results and Discussion

3.1. Physical Properties

The synthesized Gd^{3+} tellurite glasses are shown in Figure 1, where Gd_2O_3 incorporation improved the transparency and changed the color of the glass from reddish-orange to light yellow. Archimedes' principle was used to determine the density of the sample (Table 1). Physical parameters such as molecular weight and molar volume were calculated for the fabricated glasses with other parameters using the following relations.

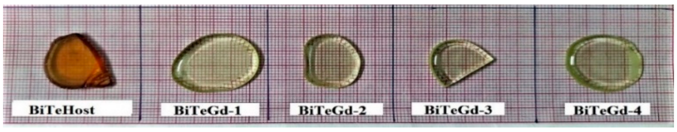

Figure 1. Pictures of synthesized BiTeGd glasses.

Table 1. Different physical parameters calculated for Gd^{3+}-doped glasses.

Sample Code	BiTeHost	BiTeGd-1	BiTeGd-2	BiTeGd-3	BiTeGd-4
Average molecular weight, M (g/mol)	159.76	161.78	163.81	165.84	167.87
Density, ρ (g/cc) (±0.01)	5.2844	5.4229	5.4429	5.4935	5.5793
Molar volume, V_m (cm^3)	30.231	29.8335	30.0967	30.1888	30.0882
Number density of Gd^{3+} ions in host glass, N_{Gd} ($\times 10^{23}$ ions/mol)	0	0.202	0.400	0.598	0.801
Inter-ionic separation between Gd^{3+}, r_i (nm)	0	36.727	29.236	25.566	23.202

For the number density of Gd^{3+} ions,

$$N_{Gd} = \frac{x N_{A\rho}}{M} \quad (1)$$

The interionic separation between Gd^{3+} ions was obtained with

$$r_i = \left(\frac{1}{N_{Gd}}\right)^{\frac{1}{3}} \quad (2)$$

All calculated parameters are summarized in Table 1. Gd^{3+} increased the density of the glass from 5.323 to 5.5793 gcm^{-3} from 0 to 4 mol% of Gd_2O_3. The high molecular weight of Gd_2O_3 compared to TeO_2 caused a density increase in the glass. The tendency of Gd^{3+} ions to form a closed-packed network by filling the interstitial spaces has also increased the density. Moreover, the Gd^{3+} ions have an ionic radius of 1.19 Å which is greater than that of Te^{4+} and Bi^{3+} ions (0.99 and 1.03 Å), which also increased the density. Molar volume (V_m) initially decreased but increased depending on the concentration of Gd_2O_3. BiTeGd-1 glass with the minimum molar volume confirmed polymerization in this glass network [8]. The number density of Gd^{3+} ions increased with the increase in Gd_2O_3 concentration. The interionic radius (r_i) decreased with successive addition of Gd_2O_3 molecules, indicating the shrinkage of ionic clouds due to Gd^{3+} ions.

The XRD images of the Gd^{3+} glasses are shown in Figure 2a. Sharp crystalline peaks were absent in the XRD images, assuring the amorphous nature of the current glasses. In addition, the broad hump observed in Bragg's angle of 20–30° also reflected the noncrystallinity of the glasses. The surface morphology of Gd^{3+}-doped tellurium borosilicate glass BiTeGd-2 was examined by using SEM images (Figure 2b).

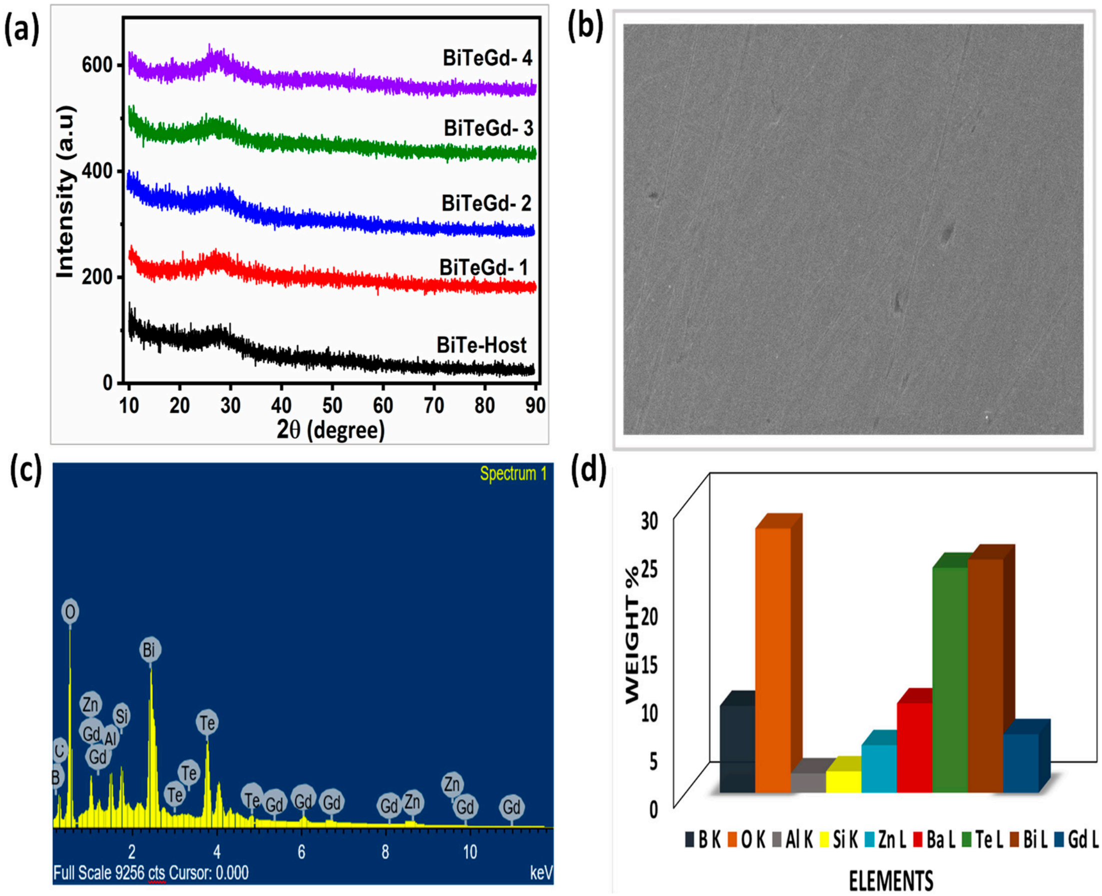

Figure 2. (**a**) XRD profiles, (**b**) SEM micrograph, (**c**) EDAX record, and (**d**) chart representing weight percentage of all the constituent elements in BiTeGd-2 glass.

The occurrence of smooth and homogenous texture in the SEM images without any cluster of unresolved particles proved the amorphous character of the synthesized glasses. The compositional analysis of the BiTeEu-2 glass was performed using EDAX measurement. The EDAX spectrum shows properly distributed elements such as boron (B), oxygen (O), silicon (Si), europium (Eu), tellurium (Te), bismuth (Bi), barium (Ba), and zinc (Zn) (Figure 2c). Aluminium (Al) was detected in the glass composition because of the alumina crucible used in the glass melting process. A bar chart representing the weights of all constituent elements (Figure 2d) exhibited the highest weight of Bismuth (Bi) as Bi has the heaviest atomic weight.

3.2. Optical Properties

The function of Gd^{3+} ions in enhancing the optical properties of the glass was studied by calculating parameters such as refractive index (n), dielectric constant (ε), molar refractivity (R_m), reflectance loss (R in %), and molar electron polarizability (α_m) [9] using the following set of equations.

$$\varepsilon = n^2 \tag{3}$$

$$R_m = \left(\frac{n^2-1}{n^2+2}\right)V_m \tag{4}$$

$$R = \left(\frac{n^2 - 1}{n^2 + 2}\right)\% \quad (5)$$

$$\alpha_m = \frac{3}{4\pi N_A} R_m \quad (6)$$

The values are presented in Table 2. The refractive index continuously increased with doping Gd_2O_3. The refractive index was influenced by a larger atomic radius (1.79 Å) of Gd [10] which is greater than that of tellurium (1.6 Å) and boron (0.98 Å). The higher polarization ability of cations resulting from higher cation radius of Gd^{3+} ions induces high *n* values, providing a platform for current Gd^{3+}-doped glasses in the non-linear optical application. An enhanced refractive index was also associated with a high dielectric constant, molar refractivity, reflectance loss, and molar electron values as shown in Table 2.

Table 2. Optical parameters of Gd^{3+}-doped glasses.

Sample Codes	R. I n	Dielectric Constant ε	R_m (cm^3)	R (%)	Molar Electron Polarizability ε_m ($Å^3$)	Band Gap E_g (eV)
BiTeHost	1.975	3.901	14.7544	0.9508	5.854	3.153
BiTeGd-1	1.989	3.955	14.8053	0.9778	5.875	2.957
BiTeGd-2	1.991	3.9663	14.9635	0.9832	5.938	3.121
BiTeGd-3	1.998	3.9939	15.0792	0.9969	5.984	3.196
BiTeGd-4	2.01	4.0407	15.1455	1.0204	6.01	2.791

The absorption spectra recorded in the UV-visible region for the Gd-doped glasses are shown in Figure 3a. The synthesized glasses including the undoped glass showed maximum absorption in the UV region (300–400 nm). In addition, all the glasses showed a broad low intense absorption peak around 500 nm which corresponds to the absorption of Bi^{3+} ions. Higher transmittance observed in the visible of all samples was proof of improved transparency of the Gd-doped glass.

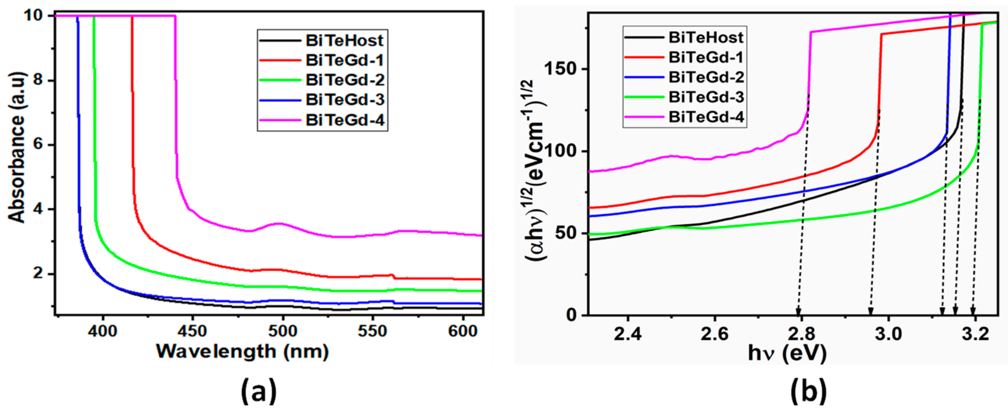

Figure 3. (**a**) UV-visible absorption spectra and (**b**) Tauc's plots drawn for BiTeGd glasses.

The relationship between absorbance and optical band gap E_g was provided by Tauc's relation as follows.

$$\alpha = \frac{B\left(h\nu - E_g\right)^{\gamma}}{h\nu} \quad (7)$$

where α is the absorption coefficient, also given by α = 2.303 A/t, A is the absorbance, t is the thickness of the sample material, B is the band tailing parameter, and the exponent γ depends on the kind of electronic transition mechanism. Because glasses are amorphous, we took γ = 2 as the transitions are indirect in nature. The resulting Tauc plot is represented in Figure 3b, where the extrapolation of the linear part of the curve is taken as E_g (Table 2).

The E_g values showed that the band gap of Gd^{3+}-doped glass was less than that of the undoped glass except for the BiTeGd-3 sample.

3.3. Radiation Shielding Parameters

MAC and HVL data simulated by Phy-X/PSD software in the 0.015–15 MeV photon energy spectrum are represented in Figure 4 [7,10]. The influence of energy on the MAC values of the glass was evident from the rapidly falling trend in the lower energy range, constancy in the intermediate range, and an increase at the higher end of the spectrum. This showed the occurrence of photoelectric absorption, Compton scattering, and electron–positron pair formation in the three energy regions. The two sharp peaks at 0.035 and 0.1 MeV were the K-edges associated with Te and Bi. Furthermore, the effect of varying the Gd_2O_3 content in MAC graphs on the continuous increase in MAC with the Gd^{3+} content was studied. Such an effect was observed because of the increasing density values of Gd_2O_3 from 5.323 to 5.579 gcm^{-3} from 0 to 4 mol% in concentration. Therefore, BiTeGd-4 glass exhibited the maximum attenuation compared to other Gd glasses.

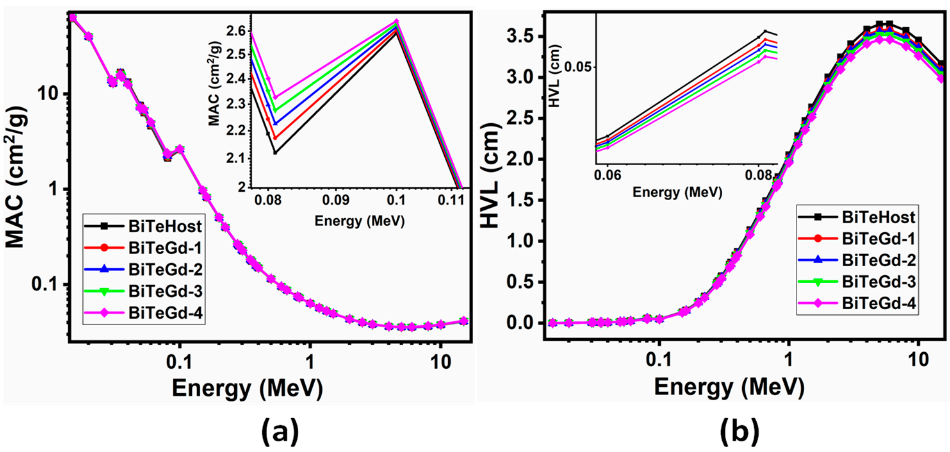

Figure 4. (**a**) MAC and (**b**) HVL of BiTeGd glasses simulated for energies in 0.015–15 MeV range using Phy-X/PSD software.

In Figure 4b, low-energy photons generated low HVL values due to the high photon absorption mechanism. HVL increased continuously in the energy range of 0.1–5 MeV, showing the maximum value at 5 MeV and a decrease to the energy of 15 MeV. This implied that when the energy increased, the radiation penetrated deeper into the glass, and therefore it was essential to increase the thickness of the material to shield it from the high radiation photons. The maximum HVL was found at 5 MeV for BiTeGd-4 glass as 3.4619 cm, which was thick enough to protect the glass from high-energy radiation. Additionally, the HVL decreased with successive doping of Gd_2O_3 in the range of 0.015–15 MeV suggesting that BiTeGd-4 glass had the lowest HVL.

4. Conclusions

Improved transparency with enhanced density values was proved with tellurite glasses doped with Gd_2O_3. Non-crystalline nature and smooth glass surface morphology were verified by XRD and FESEM results. Optical parameters including the refractive index continuously increased with an increase in Gd_2O_3. MAC and HVL parameters computed by PSD software in the energy range of 0.015–15 MeV showed that BiTeGd-4 was the optimum glass for gamma radiation shielding.

Author Contributions: Writing and data collection: A.N.D.; review and interpretation: M.I.S.; conceptualization and supervision: S.D.K. All authors have read and agreed to the published version of the manuscript.

Funding: The authors have not received any funding support for the research.

Institutional Review Board Statement: Not applicable.

Informed Consent Statement: Not applicable.

Data Availability Statement: All data generated or analyzed during this study are included in this published article.

Acknowledgments: One of the authors, Ashwitha Nancy D'Souza, expressed their gratitude to the Manipal Academy of Higher Education for providing a Ph.D. research fellowship (TMA Pai Fellowship).

Conflicts of Interest: The authors declare that there are no conflicts of interest.

References

1. Al-Hadeethi, Y.; Sayyed, M.I. Effect of Gd_2O_3 on the radiation shielding characteristics of Sb_2O_3–PbO–B_2O_3–Gd_2O_3 glass system. *Ceram Int.* **2020**, *46*, 13768–13773. [CrossRef]
2. Azianty, S.; Yahya, A.K. Enhancement of elastic properties by WO_3 partial replacement of TeO_2 in ternary $(80 - X)TeO_2$-20PbO-xWO_3 glass system. *J. Non-Cryst. Solids* **2013**, *378*, 234–240. [CrossRef]
3. Azlan, M.N.; Eevon, C.; Halimah, M.K.; El-Mallawany, R.; Hii, S.L. Effect of Gd^{3+} on optical and thermal properties of tellurite glass. *J. Theor. Appl. Phys.* **2020**, *14*, 137–147. [CrossRef]
4. Kaewjaeng, S.; Wantana, N.; Kothan, S.; Rajaramakrishna, R.; Kim, H.J.; Limsuwan, P.; Kaewkhao, J. Effect of Gd_2O_3 on the radiation shielding, physical, optical and luminescence behaviors of Gd_2O_3–La_2O_3–ZnO–B_2O_3–Dy_2O_3 glasses. *Radiat. Phys. Chem.* **2021**, *185*, 109500. [CrossRef]
5. Gaylan, Y.; Bozkurt, A.; Avar, B. Investigating Thermal and Fast Neutron Shielding Properties of B_4C-, B_2O_3-, Sm_2O_3-AND Gd_2O_3-doped Polymer Matrix Composites using Monte Carlo Simulations. *Süleyman Demirel Üniversitesi Fen Edebiyat Fakültesi Fen Dergisi* **2021**, *16*, 490–499. [CrossRef]
6. D'Souza, N.A.; Padasale, B.; Murari, M.S.; Karunakara, N.; Sayyed, M.I.; Elsafi, M.; Al-Ghamdi, H.; Almuqrin, A.H.; Kamath, S.D. TeO_2 for enhancing structural, mechanical, optical, gamma and neutron radiation shielding performance of bismuth borosilicate glasses. *Mater. Chem. Phys.* **2023**, *293*, 126657. [CrossRef]
7. Şakar, E.; Özpolat, Ö.F.; Alım, B.; Sayyed, M.I.; Kurudirek, M. Phy-X/PSD: Development of a user friendly online software for calculation of parameters relevant to radiation shielding and dosimetry. *Radiat. Phys. Chem.* **2020**, *166*, 108496. [CrossRef]
8. Gökçe, M.; Koçyiğit, D. Structural and optical properties of Gd^{+3} doped Bi_2O_3-GeO_2 glasses and glass-ceramics. *Mater. Res. Express* **2018**, *36*, 4620–4625. [CrossRef]
9. Wagh, A.; Raviprakash, Y.; Upadhyaya, V.; Kamath, S.D. Composition dependent structural and optical properties of PbF_2-TeO_2-B_2O_3-Eu_2O_3 glasses. *Spectrochim. Acta Part A Mol. Biomol. Spectrosc.* **2015**, *151*, 696–706. [CrossRef] [PubMed]
10. Samanta, B.; Dutta, D.; Ghosh, S. Synthesis and different optical properties of Gd_2O_3 doped sodium zinc tellurite glasses. *Phys. B Condens. Matter* **2017**, *515*, 82–88. [CrossRef]